2-2014

Energy Harvesting from Atmospheric Variations - Theory and Test

John Wagner
Clemson University, jwagner@clemson.edu

Gibran Ali
Clemson University

David Moline
Clemson University

Todd Schweisinger
Clemson University

Energy Harvesting from Atmospheric Variations - Theory and Test

Gibran Ali
Clemson University
Clemson, SC 29634, USA
gali@g.clemson.edu

John Wagner, PhD, PE
Clemson University
Clemson, SC 29634, USA
jwagner@clemson.edu

David Moline
Clemson University
Clemson, SC 29634, USA
moline@clemson.edu

Todd Schweisinger, PhD, PE
Clemson University
Clemson, SC 29634, USA
todds@clemson.edu

Abstract

The last two decades have offered a dramatic rise in the use of digital technologies such as wireless sensor networks that require small isolated power supplies. Energy harvesting, a method to gather energy from ambient sources including sunlight, vibrations, heat, etc., has provided some success in powering these systems. One of the unexplored areas of energy harvesting is the use of atmospheric temperature variations to obtain usable energy. This paper investigates an innovative device to extract energy from atmospheric variations using ethyl chloride filled mechanical bellows. The apparatus consists of a bellows filled with ethyl chloride working against a spring in a closed and controlled environment. The bellows expand/contract depending upon the ambient temperature and the energy harvested is calculated as a function of the bellows' length. The experiments showed that 6 J of energy may be harvested for a $23°C$ change in temperature. The numerical results closely correlated to the experimental data with a deviation of 1%. In regions with high diurnal temperature variation, such an apparatus may yield approximately $250\mu W$ depending on the ambient temperature range.

***Keywords*—** Energy harvesting, Mechatronics, Thermodynamics, Kinetics, Experimental testing

Nomenclature List

a	Area of a single thermoelectric couple (m^2)
A	Area (m^2), Riedel equation constant
B	Riedel equation constant
C	Riedel equation constant
c	Specific heat $\left(\frac{J}{kgK}\right)$, Damping constant $\left(\frac{Ns}{m}\right)$

D Diameter (m), Riedel equation constant

E Riedel equation constant

e Euler's number

F Force (N)

h Heat transfer coefficient $\left(\frac{W}{m^2K}\right)$

I Current (A)

K Thermal conductivity $\left(\frac{W}{mK}\right)$

k Spring constant $\left(\frac{N}{m}\right)$

L Length of thermoelectric couple (m)

m Mass of the middle plate (kg)

N Number of couples per module

n Number of moles, Number of terms

P Pressure inside bellows (bar)

PE Potential energy (J)

q Heat flux $\left(\frac{W}{m^2}\right)$

$\dot{q}$ Heat transfer rate (W)

R Resistance (Ω), Universal Gas Constant $\left(\frac{J}{K.mol}\right)$

S Combined Seebeck coefficient $\left(\frac{V}{K}\right)$

T Temperature (K)

t Time (s)

V Volume (m^3), Voltage (V)

x Displacement of bellows (m)

Γ Proportionality constant $\left(\frac{N}{mK}\right)$

ΔT Temperature difference ($^\circ C$)

Λ Compression of bellows & spring at $20^\circ C$ (m)

λ Length of the bellows (m)

ρ Density $\left(\frac{kg}{m^3}\right)$

Subscripts

ar Air inside the bellows

n n-type semiconductor

p p-type semiconductor

rs Restoring force

sb bellows' spring

se	External spring
t	Total
0	Free length of the bellows, Atmosphere
1	Cold side of thermoelectric
2	Hot side of thermoelectric
3	Outer heat sink
4	Inner heat sink
5	Air enclosed in the acrylic tube
6	Metal frame
7	Bellows
8	Acrylic tube
9	Ethyl chloride

1 Introduction

The field of electronics and wireless communication has witnessed many innovative trends over the decades. The size and power consumption of wireless devices has consistently reduced and the life span has seen regular growth. An ongoing challenge is to make power sources that match the life span and size of these devices, some of which need to be self-sufficient for their entire operating period as they may be located in remote or inaccessible regions. These constraints make the use of conventional power sources somewhat impractical. Traditionally, batteries, which are non-regenerative power sources, have been used to power such devices but they require frequent replacement and suffer from weight constraints. New generation micro-batteries increase the power density of the devices so that they can store enough energy to last complete life cycles. Other non-regenerative power sources such as micro-turbines and micro-heat engines, have also been used that may store chemical energy in the form of fuel which is slowly consumed over the system's lifetime. Even though the power densities of such devices have considerably improved, the energy available is always small and limited [1].

To overcome the disadvantage of having limited energy available, several regenerative power supplies have been developed. These power supplies "feed off" the environment capturing sufficient energy to operate the attached device. This method of utilizing ambient energy is called "energy scavenging" or "energy harvesting." Table 1 shows a comparison of different sources of energy and the amount of power that can be harvested using current technology. Cook-Chennault *et al* [1], Edgar [2], and Chalasani and Conrad [3] have discussed in detail the state of energy harvesting from different sources and their corresponding energy densities. Most energy harvesters can be classified into three categories based on the form of energy they

capture.

Solar Energy: Solar energy harvesters use photovoltaic cells to convert energy from ambient light to electric voltage. These are widely used for outdoor applications in places that receive ample sunlight all year round [4].

Vibrations and Kinetic Energy: These harvesters gather energy from mechanical vibrations and transduce it to an output voltage using a piezoelectric, electromagnetic or electrostatic converter. These harvesters are widely used at locations that have a source of mechanical excitation such as a vibrating machine or vibration-inducing airflow [1].

Thermal Energy: Thermal energy harvesters are generally classified in two categories. The first type utilizes Peltier effect to generate a voltage output from a temperature gradient, whereas the second type utilizes thermodynamic expansion or phase change for generating useful energy from a heat source. The energy harvester being discussed in this paper falls under the second category [2].

The focus of this research was to explore thermal energy harvesting through thermodynamic expansion of a substance in a closed system, using temperature changes in the atmosphere. If a substance is hermetically sealed in a bellows or a piston cylinder arrangement, the temperature change could be used to obtain useful work from the expansion. The expansion is most prominent when the substance changes phase. Therefore, ethyl chloride, with its normal boiling point of $287K$ was ideal for such an application as the average diurnal temperature variation would be sufficient to vaporize and condense it.

The principle of utilizing atmospheric temperature and pressure variations was first used by Cornelis Drebble in the early 17^{th} century and later more extensively by Jean-Léon Reutter when he designed the Atmos clock [5] [6]. The Atmos clock was the first device to use ethyl chloride as the working substance to power the escapement and discretize the passage of time [7] [8]. These clocks are highly efficient devices with a $1°C$ change in temperature sufficient for two days of operation [2] [9].

The experiment discussed in this paper, illustrated in Figure 1, uses a hermetically sealed brass bellows to contain ethyl chloride. As the ethyl chloride was heated/cooled by the temperature change, the length of the bellows simultaneously increased/decreased. To restrict the total expansion of the bellows and to have a quantifiable measure of output energy, an external spring was used. As the ethyl chloride cooled with the drop in ambient temperature, the bellows shrank to its original length because of the decrease in its internal pressure. The work done by the bellows' extension and contraction could now be easily measured using the spring's stiffness and contraction.

The brass bellows was attached to the base plate of a metal frame. The top and bottom plates were fixed to each other using four rods and the middle plate was mounted on linear bearings and could slide as the

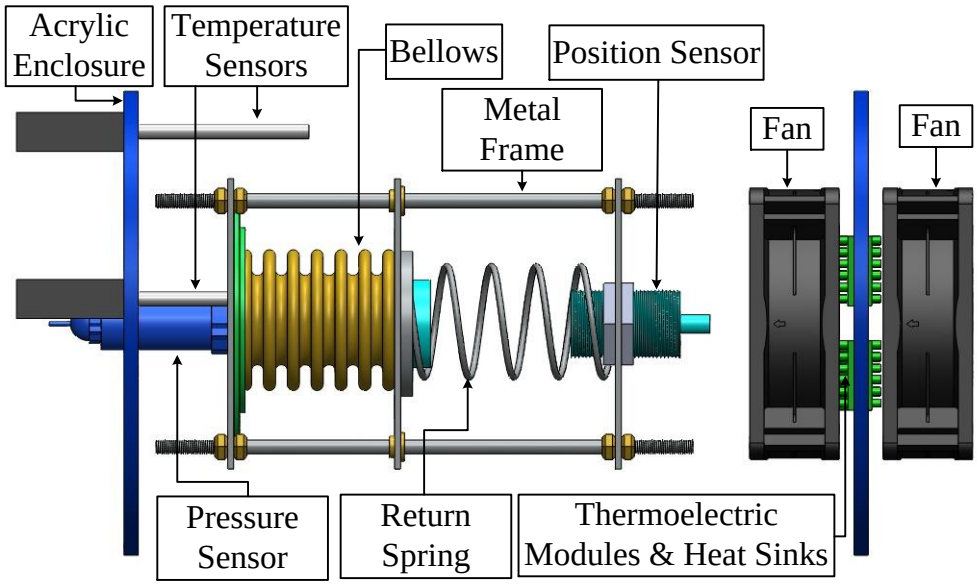

Figure 1: Energy harvesting system with accompanying sensors and actuators for bench top experiment without the acrylic enclosure

bellows expanded or contracted. To provide a force against the bellows' extension, a coiled spring was placed between the top and middle plates of the frame. A position sensor was located on the top plate to measure the displacement of a magnet attached to the top of the bellows.

The experiment was performed on a bench top in a controlled environment laboratory and the temperature variation for the system was simulated using thermoelectric modules which made the alternate heating and cooling convenient and controllable. The system can be switched between heating and cooling by changing the polarity of the applied voltage. The heat or cold from the thermoelectric modules was supplied into the system with the help of multiple heat sinks and fans. The entire system was enclosed in an acrylic tube with the thermoelectric modules attached at an end plate. The acrylic tube allowed the model to be treated as a closed system with negligible mass transfer. On the basis of this configuration, the main system elements include thermoelectric modules, heat sinks, air inside the tube, bellows with ethyl chloride and metal frame with spring.

2 Mathematical Model

The lumped parameter mathematical model describes the process of energy harvesting using the experimental configuration which has been depicted in Figure 2. Heat was added to or removed from the system by the thermoelectric modules with heat sinks. Three fans offered forced convective heat transfer which eventually resulted in changing the magnitude of potential energy stored in the mechanical spring. The complete process was divided into four subsystems and each one was analyzed individually with attention focused on the coupling factors. To simplify the system analysis, six fundamental assumptions were imposed:

Table 1: Approximate power that may be harvested from different sources; †For areas with high diurnal temperature variation [1] - [3] [10] [11] [12].

Energy Source		Characteristics	Harvested Power
Solar	Outdoor	Uncontrollable, Predictable	$15\left(\frac{mW}{cm^2}\right)$
	Indoor	Uncontrollable, Predictable	$100\left(\frac{\mu W}{cm^2}\right)$
Vibration	Piezoelectric Method	Uncontrollable, Unpredictable	$500\left(\frac{\mu W}{cm^2}\right)$
	Electromagnetic Method	Uncontrollable, Unpredictable	$4\left(\frac{\mu W}{cm^2}\right)$
	Electrostatic Method	Uncontrollable, Unpredictable	$3.8\left(\frac{\mu W}{cm^2}\right)$
Thermoelectric	$5\,^{\circ}C$ Gradient	Uncontrollable, Predictable	$100\left(\frac{\mu W}{cm^2}\right)$
	$30\,^{\circ}C$ Gradient	Uncontrollable, Predictable	$3.5\left(\frac{mW}{cm^2}\right)$
Air Flow	Outdoor $\left(Speed \approx 8\left(\frac{m}{s}\right)\right)$	Uncontrollable, Predictable	$3.5\left(\frac{mW}{cm^2}\right)$
	Indoor $\left(Speed \leq 1\left(\frac{m}{s}\right)\right)$	Controllable	$3.5\left(\frac{\mu W}{cm^2}\right)$
Ambient Radio Frequency	Transmitter Nearby ($\approx 30cm$)	Controllable	$3.5\left(\frac{mW}{cm^2}\right)$
	Transmitter Faraway	Uncontrollable, Unpredictable	$< 1\left(\frac{\mu W}{cm^2}\right)$
Electromagnetic Wave	Electric Field = $1\left(\frac{V}{m}\right)$	Uncontrollable, Unpredictable	$0.26\left(\frac{\mu W}{cm^2}\right)$
Acoustic	Noise = $100(dB)$	Uncontrollable, Unpredictable	$960\left(\frac{nW}{cm^2}\right)$
Atmospheric Variation	Temperature Change $\Delta T = 23\,^{\circ}C$	Uncontrollable, Predictable	$6(J)$, $15\left(\frac{\mu W}{cm^2}\right)$†

A1: The temperature of all the system components is time variant but spatially invariant, i.e., a lumped capacitance heat transfer model is used.

A2: The net mass transfer between the acrylic tube and the surrounding atmosphere was assumed to be zero, i.e., no air leaks

A3: The net mass transfer of ethyl chloride between the bellows to the acrylic tube was assumed to be zero, i.e., no gas leakage.

A4: The frictional effects are minimal and are lumped with the viscous damping.

A5: The external and bellows springs are assumed to be linear for whole range of prescribed motion; any non-linearities are ignored.

A6: Only convective heat transfer is considered, as the radiative part is small and the conductive part is limited to heat sinks, which are assumed to have the same temperature as the thermoelectric modules.

As the rate of temperature change within the system is slow, the acrylic tube and bellows are sealed, and the fans circulate the air inside it, these assumptions are deemed acceptable.

2.1 Thermoelectric Devices

Thermoelectric modules supply heat or cooling to the system through Peltier effect. A thermoelectric couple is composed of a p and an n-type semiconductor. When current is passed through it, one junction is heated while the other is cooled, depending on the direction of the current. A thermoelectric module typically consists of N couples. The heat generated and absorbed at the two ends is a result of three effects. First, the Peltier effect is responsible for producing the temperature gradient. Second, Joule's Law causes the couple to heat up as current passes through it. And finally, heat is conducted from the hot junction to the cold junction due to the temperature gradient between the two.

During the heating phase, the equations governing the rate of heat absorbed at the outer (cold) side, $\dot{q}_{13}$, and the rate of heat generated at the inner (hot) side, $\dot{q}_{24}$, of the module are the result of the interaction between these phenomenon so that

$$\dot{q}_{13} = 2N\left(SIT_1 - \frac{1}{2}I^2R\frac{L}{a} - K_1\frac{a}{L}(T_1 - T_2)\right) \tag{1}$$

$$\dot{q}_{24} = 2N\left(SIT_2 + \frac{1}{2}I^2R\frac{L}{a} - K_2\frac{a}{L}(T_1 - T_2)\right) \tag{2}$$

During the cooling phase, the sign for the second term is reversed making the outer side, the hot side and the inner side, the cold side. The current in the thermoelectric module can be expressed as

$$I = \frac{1}{R}(V - NS(T_2 - T_1)) \tag{3}$$

The combined Seebeck Coefficient constant, S, may be given by

$$S = |S_n| + |S_p| \tag{4}$$

where S_n and S_p are the individual Seebeck Coefficients of the n and p-type semiconductors forming the thermoelectric couple. The variables $\dot{q}_{13}$ and $\dot{q}_{24}$, based on the polarity of the applied voltage, alternately

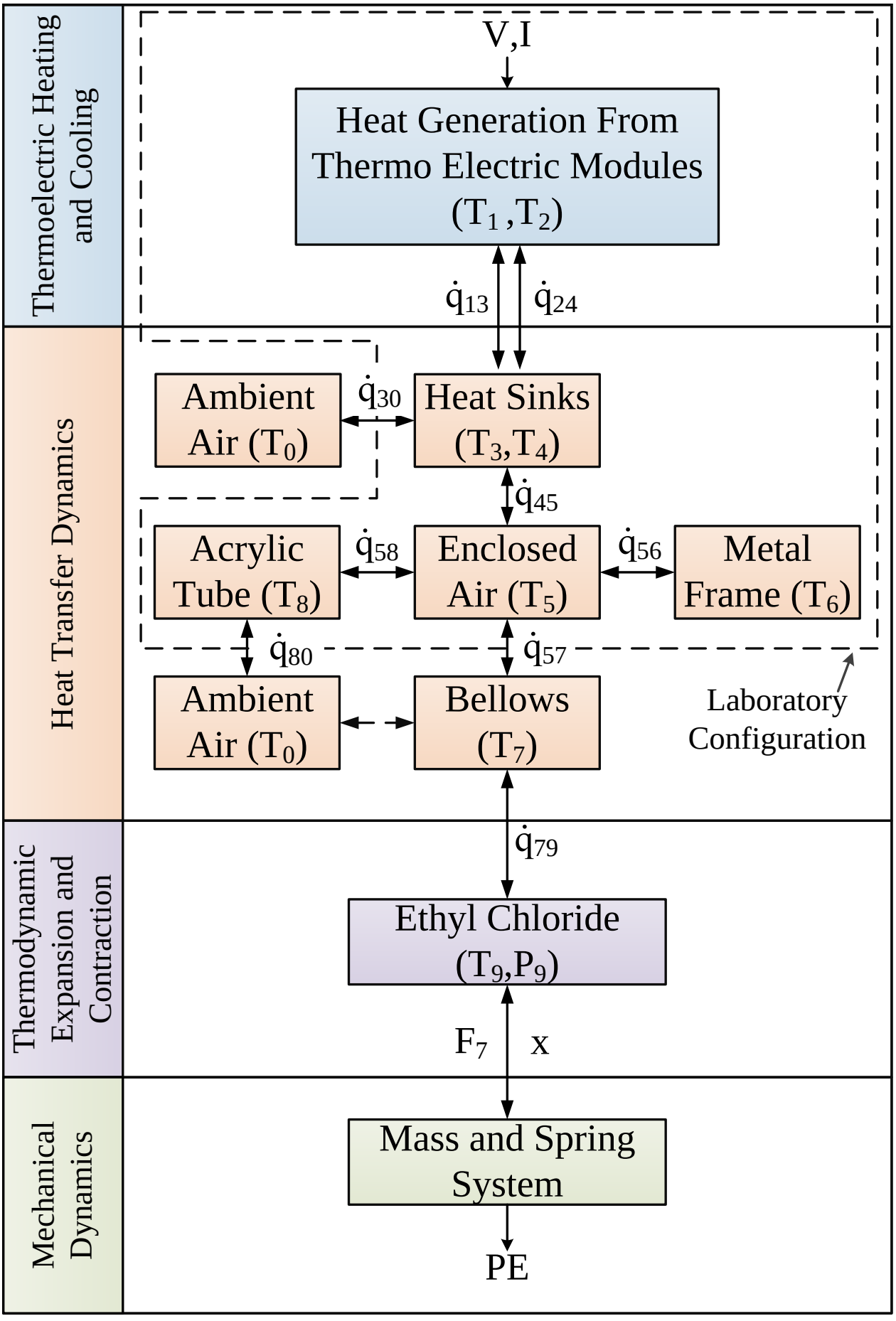

Figure 2: Energy flow in the experimental system

heat and cool the system, thus simulating temperature variations in the atmosphere.

2.2 Heat Transfer Dynamics

The thermal response of the components contained inside the acrylic tube will be mathematically described. Both sides of the thermoelectric modules were attached to heat sinks which in turn had electric fans blowing air across them to improve the heat transfer. The heat or cool entered the system via the heat sinks and air flowed across them to warm/cool the entire air volume inside the acrylic enclosure. To simplify the analysis, the heat transfer can be divided into seven interactions as shown in Figure 2. Each of these interactions can be expressed by a set of differential equations that consider the net heat flow rates of each node and consequently calculate the rate of change of temperature in that element.

The rate of temperature change calculated using the first law of thermodynamics for a given node may be

$$\rho_j V_j c_j \frac{dT_j}{dt} = \Sigma \dot{q}_{ij} - \Sigma \dot{q}_{jk} \; ; \begin{matrix} (i = 1, 2, ..., 9) \\ (j = 1, 2, ..., 9) \\ (k = 1, 2, ..., 9) \end{matrix} \tag{5}$$

where the subscripts i, j and k represent the different system components. The terms with two subscripts denote interactions between two components while the terms with one subscript signify properties of a single component.

The individual heat transfer rates can be calculated using Newton's law of cooling as

$$\dot{q}_{ij} = h_{ij} A_{ij} \left(T_i - T_j \right); \; (i = 3, 4, ..., 9; \; j = 3, 4, ..., 9) \tag{6}$$

where i and j represent the two components between which the heat transfer is taking place. In this expression A_{ij} denotes the surface area shared between i^{th} and j^{th} component over which convective heat transfer occurs. The coefficients of heat transfer, h_{ij}, can be empirically obtained observing the temperature difference between two components when a steady heat flux is applied so that

$$h_{ij} = \frac{q_{ij}}{\Delta T} \tag{7}$$

where q_{ij} is the heat flux and ΔT is the temperature difference. Alternatively, the heat transfer coefficients can be analytically determined for the given system components.

To illustrate the expansion of equation (5), the rate of change of temperature for the inner heat sink can be stated as

$$c_4 \, \rho_4 \, V_4 \, \frac{dT_4}{dt} \; = \dot{q}_{45} \; - \; \dot{q}_{24} \tag{8}$$

where $\dot{q}_{24}$ is obtained from Equations (2). The expression for $\dot{q}_{45}$ may be stated as

$$\dot{q}_{45} = h_{45} A_{45} (T_4 - T_5) \tag{9}$$

For this study, the system temperatures and heat transfer rates are defined as

$$T_i = \begin{bmatrix} T_1 & T_2 & T_3 & T_4 & T_5 & T_6 & T_7 & T_8 & T_9 \end{bmatrix}^T \tag{10a}$$

$$\dot{q}_{ij} = \begin{bmatrix} \dot{q}_{13} & \dot{q}_{24} & \dot{q}_{30} & \dot{q}_{45} & \dot{q}_{56} & \dot{q}_{57} & \dot{q}_{58} & \dot{q}_{79} & \dot{q}_{80} \end{bmatrix}^T \tag{10b}$$

All of the heat transfer relations for the components displayed in Figure 2 can be similarly derived using equations (5), (6) and (7).

2.3 Thermodynamics

As the heat from thermoelectric modules reached the saturated mixture of ethyl chloride in the bellows, the vapor pressure started changing as a function of the temperature. The total pressure in the bellows can be estimated using Dalton's law of partial pressures, which considers the sum of the partial pressure of air and the partial pressure of ethyl chloride so that

$$P_t = P_{ar} + P_9 \tag{11}$$

In this expression, P_{ar} is the partial pressure of the air and P_9 is the partial pressure of the ethyl chloride. The partial air pressure P_{ar}, can be obtained from the ideal gas law as

$$P_{ar} V = nRT \tag{12}$$

where V is the volume, n is the number of moles, R is the universal gas constant, and T is the temperature. Equation (12) can be simplified for the present application to the form

$$P_{ar} = \frac{T}{\lambda} \Gamma \tag{13}$$

where λ is the extension of the bellows, T is the temperature, and Γ is a proportionality constant given by

$$\Gamma = \frac{4nR}{\pi {D_7}^2} \tag{14}$$

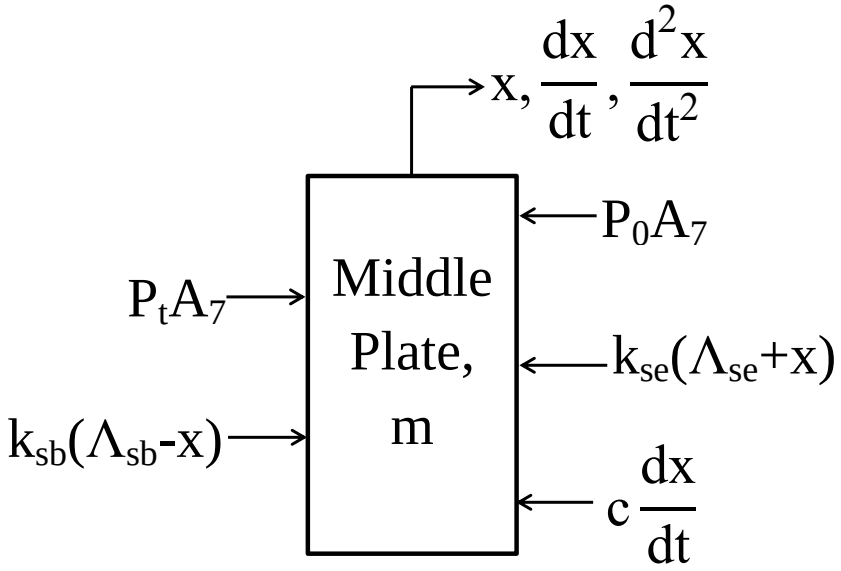

Figure 3: Free-body diagram with applied and resulting forces acting on the middle plate

The vapor pressure of ethyl chloride may be approximated using Riedel's equation as

$$P_9 = e^{\left(A+\frac{B}{T}+C\ln T+DT^E\right)} \tag{15}$$

where A,B,C,D and E are constants listed in Table 2 [13]. Although Antoine's equation can also be used to predict the vapor pressure of ethyl chloride, Riedel's equation covers the entire sub-critical temperature range, as compared to Antoine's equation which covers a much smaller range around the boiling point [14] [15] [16]. Ethyl chloride was chosen because its boiling point was within the range of temperature variation. Therefore, a small change in temperature resulted in a relatively large change in pressure when compared to other refrigerants with much higher boiling points. The ethyl chloride, C2H5Cl, mass does not affect the pressure in the bellows as long as its quantity is sufficient to maintain a saturated mixture of liquid and vapor as illustrated by equation (15). For the experiment conducted, the mass of ethyl chloride was sufficient to maintain the saturated mixture throughout the temperature variation range.

The mechanical force generated by the bellows is given by:

$$F_7 = P_t A_7 \tag{16}$$

where A_7 is the area of the bellows top.

2.4 Mechanical Dynamics

The change in pressure inside the bellows produces a force which causes an extension or contraction of the mechanical structure's length. The system was modeled as a single degree of freedom damped mass spring

system with an external force acting on it as shown in Figure 3. The system has two springs, an external spring that opposes expansion and the bellows' spring that works with the bellows' inner pressure when compressed and against it when expanded.

The equations of motion governing the system were derived using Newton's laws as follows

$$m\frac{d^2x}{dt^2} + c\frac{dx}{dt} + F_{rs} = P_t A_7 - P_0 A_7 \tag{17}$$

$$F_{rs} = (k_{se} + k_{sb})\,x + k_{se}\Lambda_{se} - k_{sb}\Lambda_{sb} \tag{18}$$

where m is the effective mass being accelerated, c is the damping constant, and Λ_{se} and Λ_{sb} are the initial compression of the external spring and bellows, respectively, at the start of the experiment.

The displacement shown is a direct indicator of the potential energy generated by the system and is given by

$$PE = \frac{1}{2}k_t x^2 \tag{19}$$

where PE is the potential energy stored in the spring. This potential energy can be harvested by a number of methods such as a piezoelectric transducer or an electromagnetic generator to power a wireless sensor node.

3 Experimental System

To validate the energy harvesting principle and explore the feasibility of thermodynamic mechanical motion, a bench-top experiment was fabricated and tested. In this section, the apparatus design and components will be discussed.

3.1 Design of Apparatus

A mechanical bellows charged with an inert gas that has a phase change at room temperature was the primary component in the energy harvesting system. The supporting elements included mechanical guides for translational motion with minimal friction, and assorted sensors and actuators to create a repeatable testing environment with measurement data. For this study, the apparatus introduced a temperature variation that influenced the ethyl chloride pressure contained in the closed system.

The bellows changed its length in response to change in pressure. To quantify the length change and to maintain an equilibrium position, a stiff coil spring resisted the bellows expansion. A metal frame, consisting of three plates and four stainless steel rods, held the apparatus in place. The two end plates were fixed to the rods using studs and nuts. The middle plate featured four linear bearings to slide along the length of the rods. The base plate and bellows were made of brass while the other plates were made of aluminum.

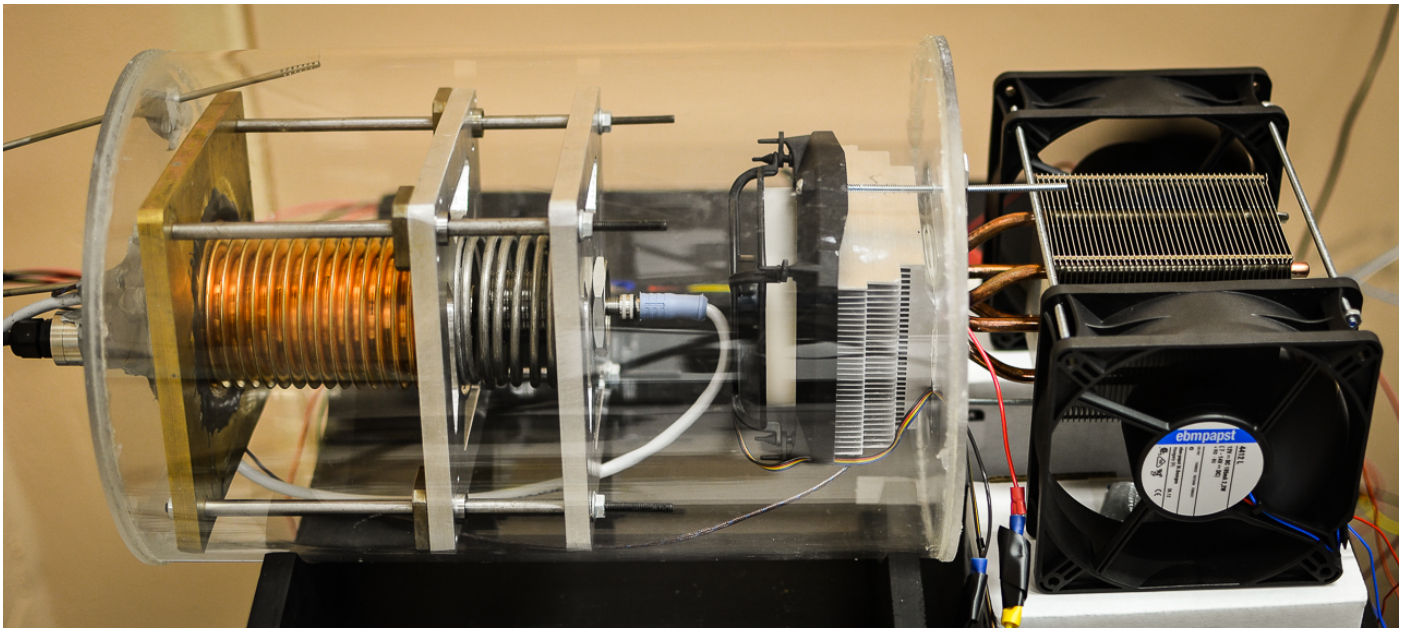

Figure 4: Assembled apparatus in protective acrylic enclosure with integrated sensors

A thermoelectric module was selected as the source of temperature variations as it could heat or cool the system. For field testing, ambient temperature changes would be sufficient to power the system. For bench top testing, cooling the system proved to be a greater challenge than heating since efficiency of thermoelectric modules are relatively low (below 15%). To improve heat dissipation on hot side, two heat sinks and three fans were used as shown in Figure 4. The outer heat sink (Dell W4254 8400) used heat pipes to achieve higher heat dissipation as its primary function was to lower the hot side temperature. The copper heat pipes connected the heat sink base to the aluminum fins. This heat sink base was attached to the thermoelectric modules and the aluminum fins were placed between two electric axial fans. A conventional, aluminum-finned heat sink, Alpine ARCTIC 64 Pro Rev. 2, with a built in electric fan, was used for the inner heat exchanger. The thermoelectric modules were connected to a 16Vold 8 Amp DC power supply.

The bellows and metal frame were mounted within an acrylic enclosure to create a closed system with negligible mass transfer. This acrylic enclosure acted as an insulator and helped in varying the temperature within reasonable time periods. The complete system was 36 cm (14 inches) long and 20 cm (8 inches) in diameter. The mechanical bellows and the metal frame assembly were 15 cm (6 inches) long and 3 inches wide.

The experimental apparatus was operated in a closed-loop manner on the bench to demonstrate the energy harvesting for temperature variations. For rising temperatures (heating phase), the thermoelectric module warmed the air inside the enclosure causing the bellows to expand. Once the gas inside the bellows reached a desired temperature, a switching circuit was activated which reversed the polarity of the thermoelectric module. The falling temperatures (cooling phase) resulted in bellows contraction. The process may

Table 2: Characteristics of experimental system components

Component Name	Property	Value (Units)
Bellows	A_7	$1.96 \times 10^{-3} \left(m^2\right)$
	A_{45}	$3.61 \times 10^{-2} \left(m^2\right)$
	k_{sb}	$876\,(N/m)$
	Γ	2.842×10^{-5}
	Λ_{sb}	$2.03 \times 10^{-2}\,(m)$
External Spring	k_{se}	$2802\,(N/m)$
	Λ_0	$2.81 \times 10^{-2}\,(m)$
Ethyl Chloride	A	44.67
	B	−4026
	C	−3.371
	c	$1.548 \times 10^{3} \left(\frac{J}{kgK}\right)$
	D	2.273×10^{-17}
	E	6
	n	0.28
	m	$18(g)$
	R	$8.314 \left(\frac{J}{K.mol}\right)$
	ρ	$9.20 \times 10^{2} \left(\frac{kg}{m^3}\right)$
Middle Plate	m	$0.2\,(kg)$
	c	$0.1 \left(\frac{Ns}{m}\right)$
Thermoelectric Module	a	$1.96 \times 10^{-6} \left(m^2\right)$
	A_{13}, A_{24}	$1.6 \times 10^{-3} \left(m^2\right)$
	K_1, K_2	$20 \left(\frac{W}{mK}\right)$
	L	$8.0 \times 10^{-4}\,(m)$
	N	199
	R	$1.5 \times 10^{-3}\,(\Omega)$
	S_n, S_p	$2.0 \times 10^{-4}\,(V/K)$
	V	$16.5\,(V)$

be repeated using the relay switch to change circuit polarity.

3.2 Sensors, Actuators and Data Acquisition

A series of sensors and actuators were integrated into the experimental system to monitor and control the apparatus. Although this hardware would not be required for energy harvesting in the field, it offers insight into overall performance, while providing a repeatable environment.

Pressure Sensor: An Omega PX309-050A5V (0 bar to 3.4 bar) pressure sensor monitored the ethyl chloride

pressure inside the bellows. This served the dual purpose of acting as a point of correlation between the numerical and experimental models and helping improve modeling the ethyl chloride pressure.

Proximity Sensor: A Micro-Epsilon MDS-45-M30-SA (0 mm to 45 mm displacement) magneto-resistive type proximity sensor measured the bellows displacement or spring position which directly correlated to the energy harvested.

Thermocouple: Three J type Omega SMP-AP-J-125E-6 (0 $^{\circ}C$ to 750 $^{\circ}C$) thermocouples measured the temperature of air inside the acrylic enclosure, ethyl chloride inside the bellows, and the inner heat sink. Amplifiers were used to amplify the thermocouple voltages to reduce noise in the measurements. The sensors were the contact thermocouples capable of measuring a temperatures from .

Fan: Three fans were used in the system. Two of these were used on the outer heat sink (Mcmaster 1939K23, 12V DC) to maximize heat dissipation. Only one fan was used on the inner side which came as a part of the heat sink package (Alpine 64 Pro) intended to be used for cooling CPU's.

Thermoelectric Module: One thermoelectric module (TE Technologies HP-100-1.4-0.8) was used to heat and cool the system. The theoretical cooling possible was 172 W at a hot side temperature of 27$^{\circ}C$.

To acquire data from the sensors, National Instruments LabVIEW was used with a PCI 6143 board. A control loop selected between heating and cooling the system. The bellows temperature was compared against predefined upper and lower limits and crossing these triggered the control loop to switch polarity. The upper and lower temperature values were set to represent realistic temperature variations in different climatic conditions at various times of the year. This helped in gaining an understanding of the energy harvesting potential of the apparatus at such locations.

4 Numerical & Experimental Results

The thermodynamic driven energy harvesting apparatus was tested for a variety of conditions in the laboratory to validate the concept. Although the ambient air temperature was maintained at $T = 22^{\circ}C$, the thermoelectric devices allowed the acrylic enclosure air to be heated or cooled as needed. Figure 5 shows the variation in temperature, pressure and position as measured in the experiment. The data illustrates the change in system values over a period of two cycles completed in 3.5 hours drawing a current of 6.5 A at 16 VDC. The ethyl chloride temperature triggered the heating/cooling loop with 33 $^{\circ}C$ as the maximum and 17 $^{\circ}C$ as the minimum temperature. The heating rate was much higher than the cooling rate due to the difference in heating and cooling efficiencies of the thermoelectric module. The expansion of the bellows was algebraically calculated from the position data which gives the position of the middle plate relative to the fixed top plate. It can be observed in Figure 5that as the ethyl chloride temperature rose above 30 °C, the bellows reached its maximum extension. This phenomenon was due to the middle plate of the metal frame

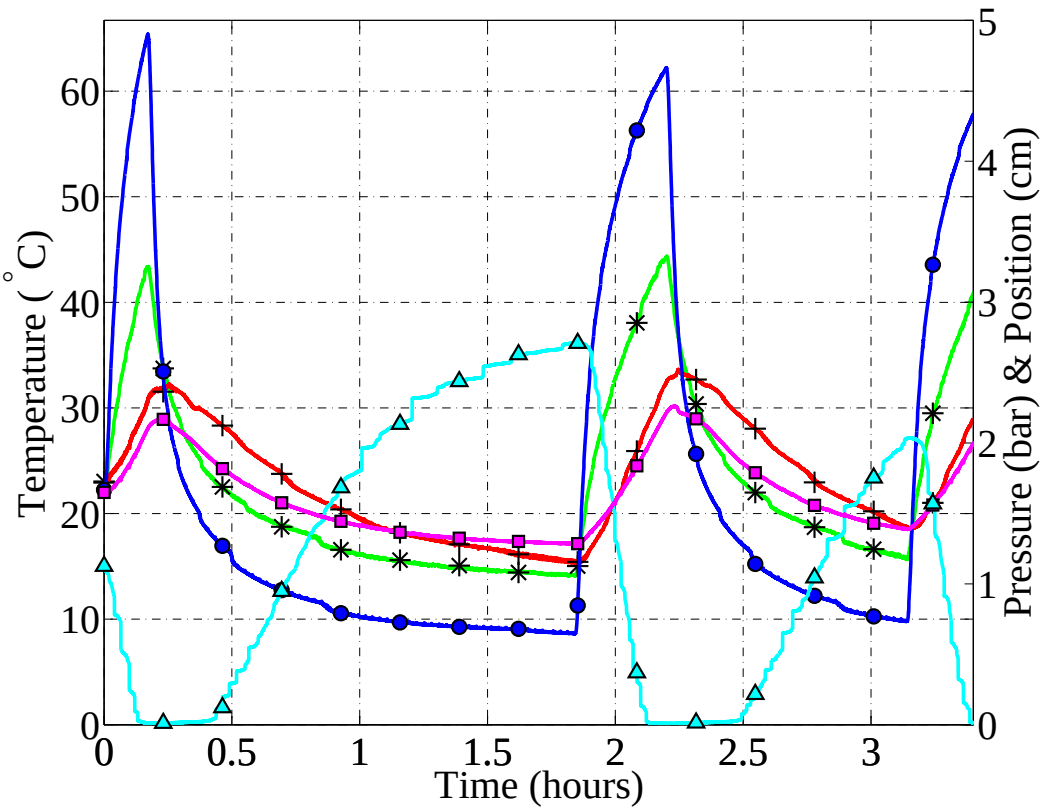

Figure 5: Experimental data acquired from the test apparatus versus time; curves are defined as: heat sink temperature (blue/circle), air temperature (green/asterisk) and ethyl chloride temperature (red/plus) in $°C$, pressure inside the bellows (magenta/square) in bar and position of middle plate (cyan/triangle) in cm.

assembly coming in contact with the position sensor. Therefore, the position data for maximum extension was ignored as it did not represent the system accurately.

The data was divided into heating, cooling and switching phases. This analysis was necessary since the thermocouple in the ethyl chloride measured temperature values at the center of the bellows. The temperature at the center was lesser, equal to or greater than the temperature towards the edges of the bellows in heating, switching and cooling phases respectively.

The data from different experiments, performed over several days, was compared and found to be satisfactorily repeatable. Figure 6 shows the variation of pressure versus temperature for simulated values and measured data. The two sets of data show similar trends with an average percentage error of 1.2%. The pressure increased from 1 bar to 2.1 bar as the temperature was increased from $5°C$ to $33°C$. The comparison of the simulated and measured position versus temperature data is shown in Figure 7. The position in this plot refers to the distance between the middle and the top plates. The expansion of the bellows was calculated by subtracting the position from the initial distance between the two plates. The "steps" observed in the measured data in Figures 5, 7 and 8 are due to the stiction between the middle plate bearings and the supporting rods. The pressure inside the bellows increased continuously with temperature, as shown in Figure 6. The net force acting on the middle plate also increases continuously and a step change in position occurs whenever

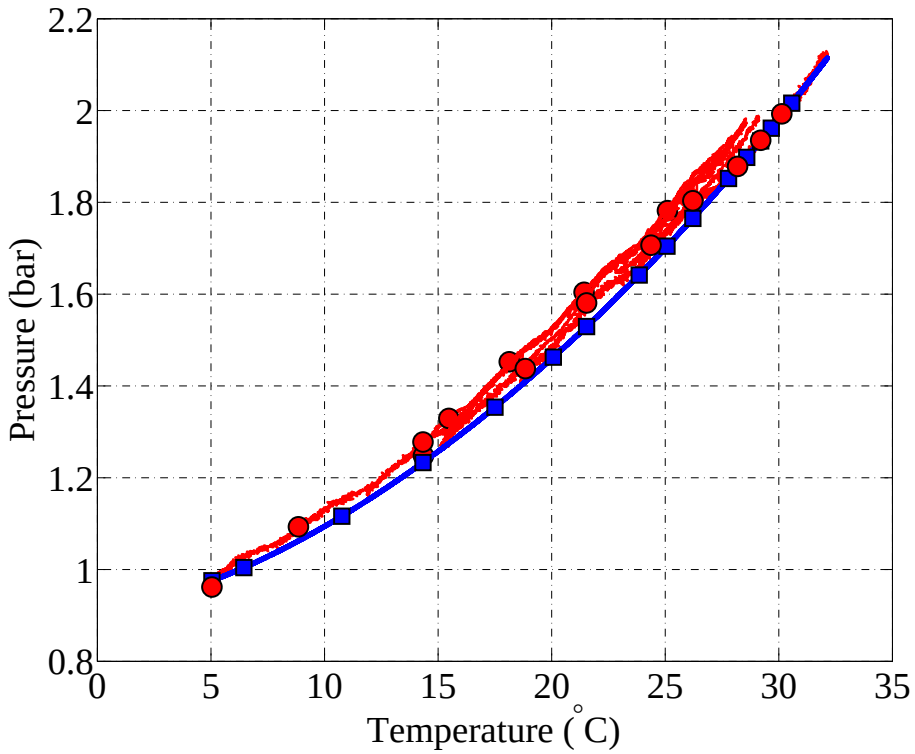

Figure 6: Experimental (red/circle) and analytical (blue/squares) pressure inside the bellows versus ethyl chloride temperature

the net force exceeds the threshold needed to overcome the stiction as displayed in Figure 7. The middle plate moved from a distance of $4cm$ at $7°C$ to $\approx 0cm$ at $29°C$.

Potential energy is stored in the external spring as the bellows expands. Figure 8 compares the simulated and measured potential energy versus temperature. Six joules of energy are stored in the spring for a temperature variation of 23°C. The potential energy is released during the cooling phase and the spring works to push the bellows back to its initial position.

It was observed from the heating phase data that the pressure and displacement changed 0.04 bar/°C, and 0.2 cm/°C and 4 cm/bar, respectively. The displacement is linearly related to the temperature and the potential energy is proportional to the second power of the temperature. This is due to the quadratic relation of potential energy and displacement as shown in equation (19).

5 Conclusion and Future Work

The concept of energy harvesting from atmospheric temperature variations was proposed and experimentally verified. A potential energy output of 6 Joules for a temperature difference of 23°C was observed which could be used in combination with a transducer to run low power electronics in remote locations. Since the amount of energy extracted is directly related to the temperature change, regions with high diurnal temperature variations would be ideally suited for such devices. For example, the southwest region of the United States experiences average diurnal temperature ranges of 30 to 40 $°C$ for many months in a year [12].

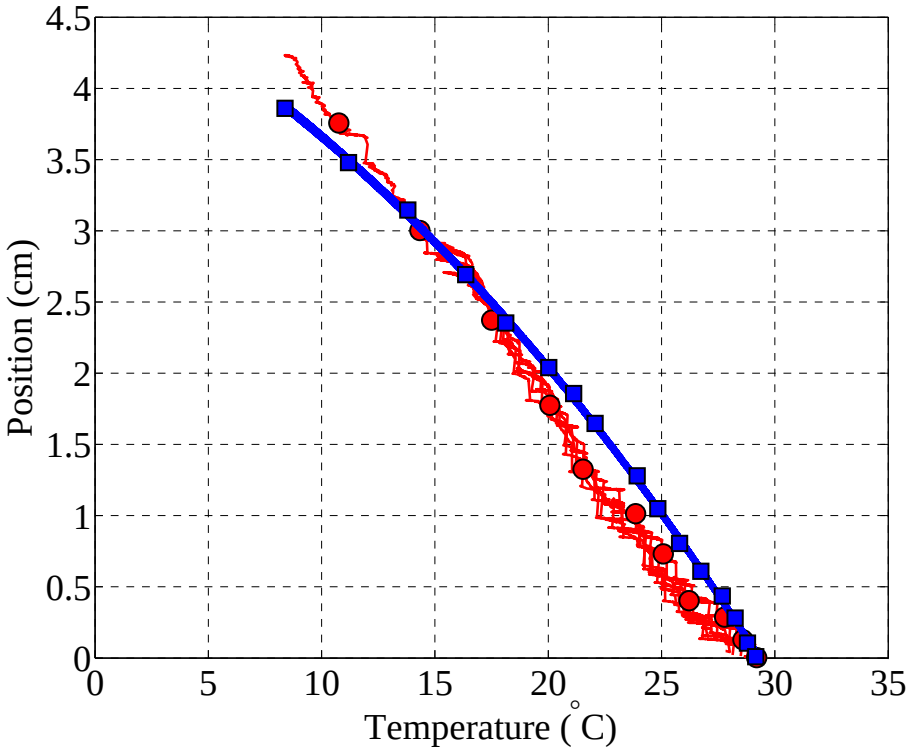

Figure 7: Experimental (red/circle) and analytically simulated (blue/square) distance between the bellows and top plate versus ethyl chloride temperature.

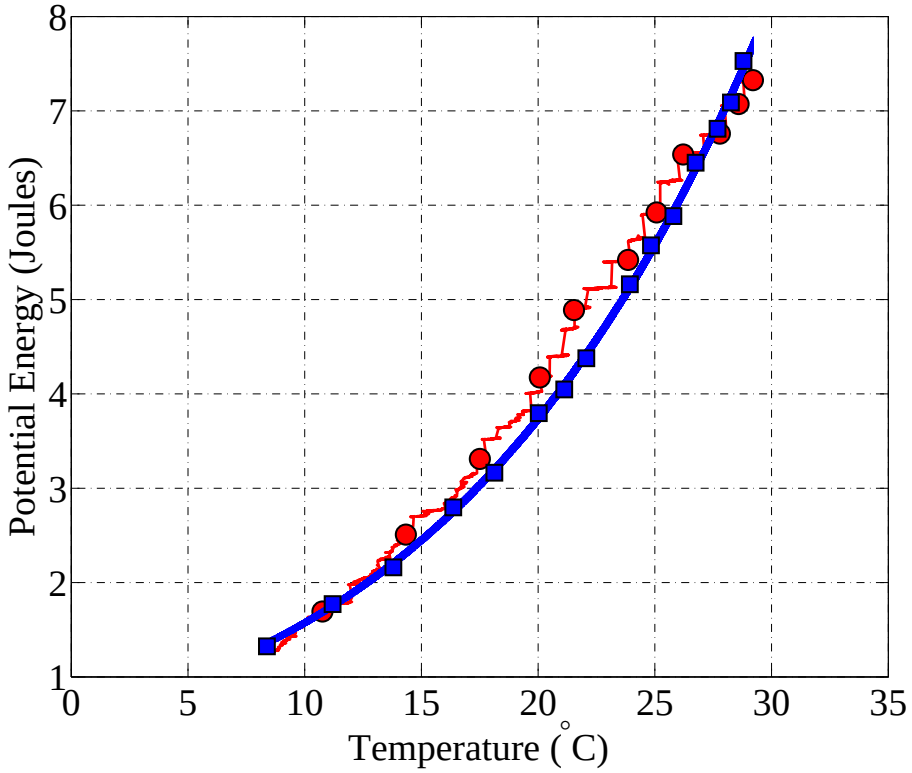

Figure 8: Measured (red/circle) and calculated (blue/square) mechanical potential energy stored in the spring versus temperature. A change of $6J$ for a temperature change of 23°C was observed.

The thermal fluctuations are ideal for the energy harvester discussed in this paper and could produce about $250\mu W$.

Future work involves the development of a micro generator that converts the energy stored in the spring into usable electrical power. A small gear-train mechanism transfers the reciprocation motion of the middle plate into unidirectional rotation of a shaft which can then wind a spiral spring. When enough energy is stored in the spiral spring, the small generator produces electricity using the potential energy.

References

[1] K. Cook-Chennault, N. Thambi, and A. Sastry, "Powering MEMS Portable Devices – A Review of Non – Regenerative and Regenerative Power Supply Systems with Special Emphasis on Piezoelectric Energy Harvesting Systems," *Smart Materials and Structures*, vol. 17, no. 4, p. 043001, 2008.

[2] C. J. H. Edgar, *Wireless Sensor Networks: Architectures and Protocols*. CRC Press: Boka Raton, FL, 2003.

[3] S. Chalasani and J. Conrad, "A Survey of Energy Harvesting Sources for Embedded Systems," in *IEEE Proceedings of the SoutheastCon*, (Huntsville, Al), pp. 442–447, April 2008.

[4] S. Sudevalayam and P. Kulkarni, "Energy Harvesting Sensor Nodes: Survey and Implications," *Communications Surveys Tutorials, IEEE*, vol. 13, no. 3, pp. 443–461, 2011.

[5] J. Lebet and F. Jequier, *Living on Air: History of the Atmos Clock*. Le Sentier, Switzerland: Jaeger-LeCoultre, 1997.

[6] Anonymous, "The Atmos Clock," *The Horological Journal*, pp. 12,16,56,58, May and June 1934.

[7] S. Patel, D. Moline, and J. Wagner, "Modeling and Analysis of an Atmospheric Driven Atmos Clock with Mechanical Escapement Control," in *2013 European Control Conference*, (Zurich, Switzerland), pp. 281–287, 2013.

[8] D. Moline, J. Wagner, and E. Volk, "Model of a Mechanical Clock Escapement," *American Journal of Physics*, vol. 80, no. 7, pp. 599–606, June 2012.

[9] R. Roerich, "Atmos-The Perpetual Clock," *Bulletin of the National Association of Watch and Clock Collectors, Inc.*, vol. 30, no. 257, pp. 494–500, December 1988.

[10] J. Paradiso and T. Starner, "Energy Scavenging for Mobile and Wireless Electronics," *Pervasive Computing, IEEE*, vol. 4, no. 1, pp. 18–27, 2005.

[11] G. Tuna, V. Gungor, and K. Gulez, "Energy Harvesting Techniques for Industrial Wireless Sensor Networks," in *Industrial Wireless Sensor Networks* (V. Gungor and G. Hancke, eds.), (Oxford), p. 125, CRC Press, 2013.

[12] D. Sun, R. T. Pinker, and M. Kafatos, "Diurnal Temperature Range over the United States: A Satellite View," *Geophysical Research Letters*, vol. 33, no. 5, p. L05705, March 2006.

[13] Design Institute for Physical Properties Sponsored by AIChE, "Ethyl Chloride." http://app.knovel.com/web/view/html/show.v/cid:kt00A3M222/viewerType:html/rid:10233891/root_slug:dippr-project-801-full/url_slug:ethyl-chloride/hid:444406184?curve_ids=kr07CLBZ21&page=1. Accessed: January 2014.

[14] J. Gordon and W. Giauque, "The Entropy of Ethyl Chloride. Heat Capacity from 18 to 287 K. Vapor Pressure, Heats of Fusion and Vaporization," *Journal of the American Chemical Society*, vol. 70, no. 4, pp. 1506–1510, 1948.

[15] Office of Response and Restoration (ORR), National Oceanic and Atmospheric Administration, U.S. Department of Commerce, "Ethyl Chloride." http://cameochemicals.noaa.gov/chris/ECL.pdf. Accessed: January 2014.

[16] National Institute of Standards and Technology (NIST), "Ethyl Chloride." http://webbook.nist.gov/cgi/cbook.cgi?ID=C75003&Units=SI&Mask=4#Thermo-Phase. Accessed: January 2014.